EDN: JTHLGC
УДК 538.9

Resonance Properties of the $Y_{0.5}Sr_{0.5}Cr_{0.5}Mn_{0.5}O_3$ Polycrystal

Mukhametkali M. Mataev*
Kazakh National Women's Teacher Training University
Almaty, Kazakhstan
Gennadiy S. Patrin†
Siberian Federal University
Kirensky Institute of Physics
Federal Research Center KSC SB RAS
Krasnoyarsk, Russian Federation
Karima Zh. Seitbekova
Abai Kazakh National Pedagogical University
Almaty, Kazakhstan
Yaroslav G. Shiyan
Siberian Federal University
Kirensky Institute of Physics
Federal Research Center KSC SB RAS
Krasnoyarsk, Russian Federation
Viktor R. Churkin
Siberian Federal University
Krasnoyarsk, Russian Federation

Received 10.06.2024, received in revised form 15.07.2024, accepted 24.09.2024

Abstract. This work presents the results of the experimental studies of the magnetic resonance properties of the $Y_{0.5}Sr_{0.5}Cr_{0.5}Mn_{0.5}O_3$ polycrystalline system. We found that two absorption lines are observed in the magnetic ordering region at $T < 80$ K in the spectrum. When changing to the paramagnetic region, one of the lines disappears, but a set of weak lines appears, which are identified as belonging to the Mn^{2+} impurity ions. The temperature behavior of the main peak line width is analyzed within the framework of the single-ion relaxation theory. Mn^{3+} ions were found to be responsible for the low-temperature peak, and Cr^{4+} ions are responsible for the high-temperature peak. The constants of the molecular fields acting on the Mn^{3+} and Cr^{4+} subsystems have been determined.

Keywords: yttrium-strontium chromite-manganite, antiferromagnetic interaction, magnetic resonance, one ionic relaxation.

Citation: M.M. Mataev, G.S. Patrin, K.Zh. Seitbekova, Y.G. Shiyan, V.R. Churkin, Resonance Properties of the $Y_{0.5}Sr_{0.5}Cr_{0.5}Mn_{0.5}O_3$ Polycrystal, J. Sib. Fed. Univ. Math. Phys., 2024, 17(6), 732–742. EDN: JTHLGC.

Introduction

At present, compounds based on various oxides are actively studied, where it is possible to obtain both purely magnetic compounds and those that belong to the class of multiferroics [1]. Inhomogeneous media with developed interfaces between mesoscopic structural elements are of great interest. Such systems are with phase separation, film structures, and nanoscale composites [2]. In this respect, compounds from the class of manganites with the $A_xB_{1-x}Mn_yMe_{1-y}O_3$

*mataev_06@mail.ru https://orcid.org/0000-0002-9057-5443
†patrin@iph.krasn.ru https://orcid.org/0000-0002-4786-0644.

general formula, where A is a rare earth element, B is usually an alkaline earth element, and Me is a 3d metal, have been studied in the most detail [3]. The base compound is $LaMnO_3$, in particular, the doping of this compound with Sr^{2+} ions depending on the impurity concentration results in a great variety of properties [4]. In mixed chromite-manganites, the effect of exchange displacement occurs due to the competition of exchange interactions between one-and dissimilar Cr and Mn ions with different valences [5–7] and the inversion effect of the magnetization sign [8]. When yttrium impurities are added instead of lanthanum, an abnormal change in the relative volume, a variety in the reverse susceptibility [9], and relaxation processes of magnetization [10] are observed, which are typical for spin glasses. In polycrystalline lanthanum-strontium manganite doped with chromium in low concentrations (8%<) a return spin-glass behavior is observed [11]. At the same time, the technology of obtaining samples has a strong influence on the properties of polycrystals. It was previously established that in the $Y_{0.5}Sr_{0.5}Cr_{0.5}Mn_{0.5}O_3$ polycrystalline sample there are two magnetic subsystems with different types of magnetic behavior, but the question of the role of different 3d elements remains open [12]. The above shows that partial replacement of both the rare earth element and the transition 3d metal significantly affects the physical properties of manganites.

Since magnetic resonance data provide some information about internal fields and interactions in magnets, we decided to investigate the magnetic resonance properties of polycrystalline yttrium-strontium chromite-manganite.

1. Material and methods

A mixture of oxides Y_2O_3, $SrCO_3$, Cr_2O_3, and Mn_2O_3 was used to obtain the $Y_{0.5}Sr_{0.5}Cr_{0.5}Mn_{0.5}O_3$ manganate. The obtained samples of complex oxides were prepared by the sol-gel method [12, 13]. The phase state of the final products was monitored by x-ray phase analysis by means of a Miniflex 600 X-ray diffractometer (Rigaku). Electron microscopic measurements were performed by a JEOL JEM-2100 microscope. Magnetic characteristics were studied on the MPMS-XL SQUID-magnetometer in fields up to 50 kOe. Electron magnetic resonance (EMR) spectra were measured by means of a EPR spectrometer ELEXSYS E580, Bruker, Germany operating at a frequency 9.48 GHz. Magnetic resonance measurements were performed in the temperature range from 5 K to 300 K.

2. Experimental

The X-ray spectroscopy method showed that the crystals correspond to the nominal composition and belong to the orthorhombic syngony with the cell parameters $a = 0.7065$ nm, $b = 0.7375$ nm, and $c = 0.6741$ nm. The density of the substance was $\rho \approx 3.95$ g/cm^3. The average size of the crystallites can be considered by the electron microscopic image in Fig. 1 ($L \geqslant 10$ μm). Local values of the chemical elements content obtained by transmission spectroscopy from spots with a diameter of $\sim$ 20 nm in different places of the sample, both in atomic content and in weight, correspond to the nominal values with an accuracy of 5–6% [12].

When measuring the resonant absorption, we found that at low temperatures the spectrum consists of two lines 1 and 2 (see Fig. 2, part a). The resonant field of a high-field line (H_{r2}) is practically independent of temperature; the intensity of this line (defined as the area under the curve and proportional to the number of absorbing centers [14]) decreases in magnitude and the line disappears at $T \approx 80$ K. This temperature coincides with the temperature identified as the temperature (T_N) of the magnetic ordering in the sample during magnetostatic measurements [12]. However, as it can be seen in Fig. 3a, this line has a relatively narrow width. Line 1 is wide and is observed over the entire temperature range studied. As the temperature rises, the line 2

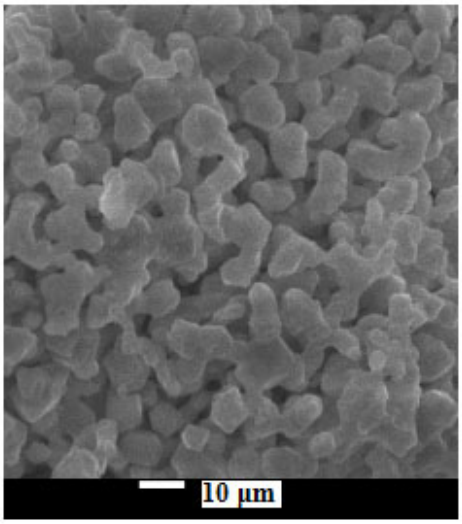

Fig. 1. The electron microscopic image of a chromite-manganite polycrystal of the $Y_{0.5}Sr_{0.5}Cr_{0.5}Mn_{0.5}O_3$ composition

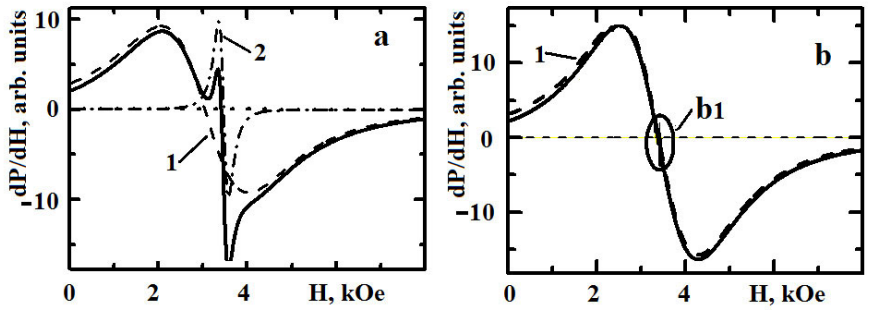

Fig. 2. The resonance absorption spectrum in the $Y_{0.5}Sr_{0.5}Cr_{0.5}Mn_{0.5}O_3$ polycrystal for temperatures (a) $T = 39$ K, (b) $T = 270$ K. The lines 1 and 2 are fitting Lorentz curves, the solid line is the experimental curve

disappears, and a set of 3 clearly seen lines appears near its location (Fig. 3, part b1), but with an extremely low intensity.

The temperature dependences of the resonant fields of microwave absorption (H_r) are shown in Fig. 4. It can be seen that the H_r values for lines 2, 3, 4, and 5 practically do not depend on the temperature over the entire range of their existence. For line 1, the dependence of the resonant field increases strongly with increasing temperature, but at $T > 80$ K, its value also becomes independent of temperature.

The behavior of the intensities (J) of absorption lines (Fig. 5, part b) at high temperatures is similar to the behavior of resonant fields. In the temperature range of the existence of line 2 ($T < 80$ K), its intensity decreases with increasing temperature, and the intensity of the main resonance (line 1), passing through the maximum at low temperatures, also becomes temperature-independent in the high temperature range.

The resonant absorption line widths (ΔH) show a more complex behavior. Lines 3, 4, and 5 are narrow and do not depend on temperature. The width of line 2 increases slightly as it

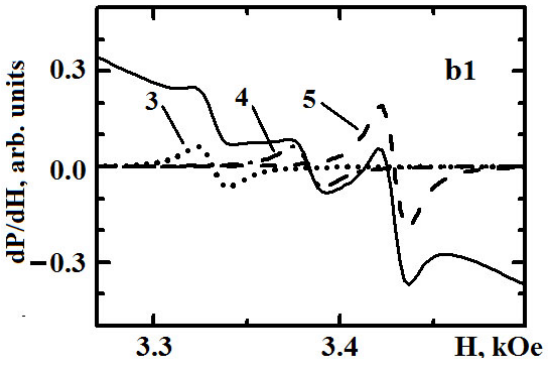

Fig. 3. The fine structure of the spectrum of the selected area in Fig. 2. The lines 3, 4, 5 are fitting Lorentz curves, the solid line is the experimental curve

approaches the temperature T_N. For line 1, ΔH has two distinct maxima. One of them is narrower and more intense in the magnetic ordering region and another is wide in the paramagnetic region.

3. Discussion

When discussing magnetic resonance properties, we use the results of magnetostatic measurements. These measurements show that individual ferromagnetic crystallites are bound together by an antiferromagnetic interaction (at $T < T_N$). It is well known [15, 16] that at the transition to the nano or micro scale a shell with a distorted structure is formed in doped manganites in the near-surface layer. With decreasing of the particle size the role of the surface layer increases. In this case, e.g. for the La-Sr-Mn-O system, the magnetization for granules larger than 200 nm coincides with the magnetization of the bulk material [17]. The temperature behavior comparison of the resonant absorption intensities (Fig. 5b, curves 1 and 2) allows us to conclude that in the region of line 2, its intensity is less than the intensity of the main line by about an order of magnitude. Line 2 (Fig. 2a) can be identified as a line belonging to the outer shell of the crystallite. Its abrupt disappearance presumably indicates that the transition is a first-order phase transition, which can be observed in systems with large granules [17].

The fine structure in Fig. 3 can be explained by the existence of the Mn^{2+} ions. Thus, it is reported [18] that the TEM method detects inhomogeneities in the shell surrounding the core of the granule which are associated with the formation of small manganese clusters. Besides, the X-ray absorption spectroscopy (XAS) method showed the presence of the Mn^{2+} ions localized on the film surface [19]. Thus, structural imperfections lead to the appearance of divalent manganese ions. Thus, the structure imperfections lead to the appearance of the divalent manganese ions.

3.1. Model representation

The features of the width of line 1 in Fig. 5a do not correspond to the behavior inherent in the ensemble of superparamagnetic particles [20, 21], where a significant widening of the absorption line at low temperatures and its narrowing at temperatures above the blocking temperature is typical. In our case, the shape of the temperature dependence ΔH is qualitatively similar to that observed, for example, in the $Mn_xFe_yO_4$ crystals [22], where the behavior of the line width is described by ion relaxation processes [23].

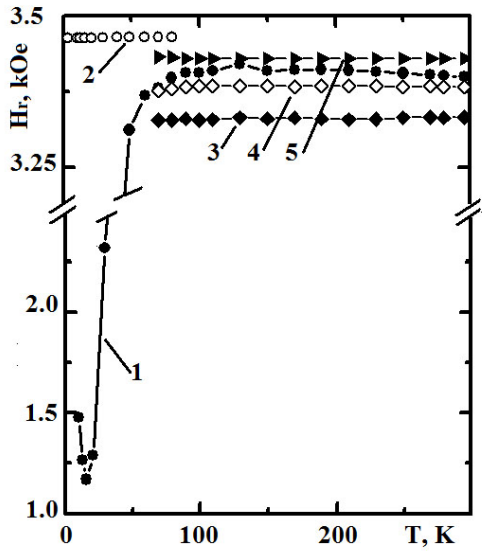

Fig. 4. The temperature dependences of resonant fields. The curve designations correspond to the lines in Fig. 2 and Fig. 3

As it is known [3], ideal manganite crystals have the structure shown in Fig. 6a. Magnetic ions occupy an octahedral position, and there is one magnetic ion per unit cell. The compound $Y_{0.5}Sr_{0.5}Cr_{0.5}Mn_{0.5}O_3$ has orthorhombic symmetry with the unit cell volume $V_{el} \approx 0.35$ nm^3, which corresponds to the total concentration of magnetic ions $N_0 \approx 2.85 \cdot 10^{21}$ cm^{-3}. In the $Y_{0.5}Sr_{0.5}Cr_{0.5}Mn_{0.5}O_3$ crystal, Mn^{4+} and Cr^{4+} ions are formed along with Mn^{3+} and Cr^{3+} ions due to the introduction of the Sr^{2+} ions. As noted above, the crystal composition corresponds to the nominal composition, it means that each type of magnetic ion corresponds to the concentration of $N_k = N_0/4 = 7.12 \cdot 10^{20}$ cm^{-3} $(k = 1, 2, 3, 4)$. The most anisotropic ions among the entire set of them are those with an even number of electrons, such as Mn^{3+} and Cr^{4+}. They can make the main contribution to the magnetic resonance line width.

The general basics of the ion relaxation theory in magnetically ordered crystals were founded by Clogston [24]. According to this theory, the width of the magnetic resonance line depends on the modulation of the energy levels of the impurity subsystem which is exchange bounded to the magnetic matrix. It is obtained that

$$\Delta H = \frac{M_0}{2} \cdot \left[\frac{\omega\tau}{1 + (\omega\tau)^2} \right] \cdot P, \tag{1}$$

where ω is the frequency of magnetization fluctuations, τ is the relaxation time of level populations, and M_0 is the magnetization and the last multiplier

$$P = -\sum_{j=1} \left(\frac{\partial n_j}{\partial \theta} \cdot \frac{\partial \varepsilon_j}{\partial \theta} + \frac{\partial n_j}{\partial \phi} \cdot \frac{\partial \varepsilon_j}{\partial \phi} \right), \tag{2}$$

where ε_j is the energy levels of impurity ions, n_j is the equilibrium populations of the levels, θ and ϕ are polar and azimuthal angles. The most effective magnetic relaxation occurs at the ratio $\omega\tau = 1$. Hereinafter, we will use this approximation.

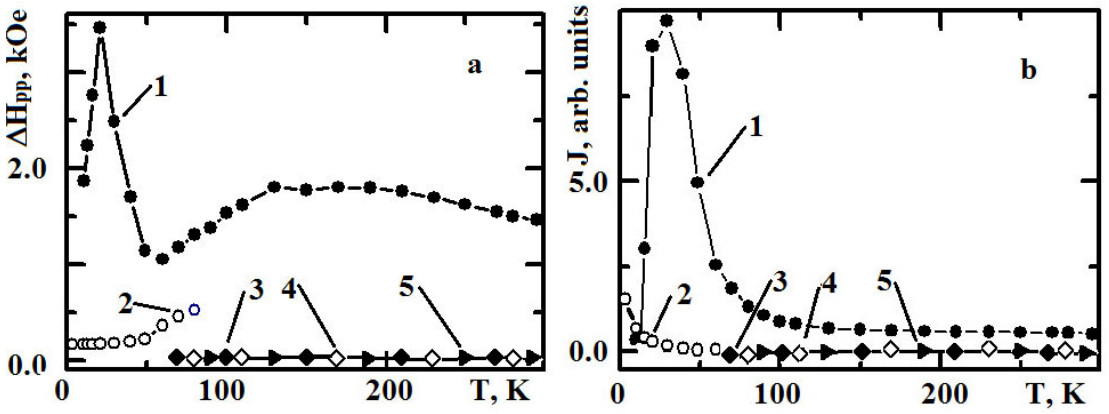

Fig. 5. The temperature dependences: a — line widths of resonant curves, b — line intensities. The curve designations correspond to the lines in Fig. 2 and Fig. 3

3.2. The low-temperature maximum

As it is known from early studies [22] the low-temperature ($T \sim$ 15–20 K) maximum of the line width in magnetically ordered manganese-containing ferrites is associated with the ionic relaxation of the Mn^{3+} ions. This ion has a $3d^4$ configuration and a 5D electron term with L = 2 and S = 2. In the crystal field of octahedral symmetry, the D-term splits into a doublet and a low-lying triplet [25], which further splits into singlets due to uniaxial distortions and the strong Jahn–Teller interaction ($E_{JT} \sim 0.25$ eV (2900 K)) [26]. As a rule, Jahn–Teller ions show strong anisotropic behavior, so for the $s = 2$ ground level ion, the Hamiltonian is written as [25]:

$$W_1 = -S_z \cdot (g_1 \cdot H + \lambda_1 \cdot M) \cdot \cos(\theta + \alpha) - D_1 \cdot \left[S_z^2 - \frac{1}{3} S(S+1) \right], \tag{3}$$

where $S_i (i = X, Y, Z)$ are spin components, H is the external magnetic field, M is the molecular field acting on the Mn^{3+} ion from all other magnetic ions, D_1 is the crystal field parameter, θ is the angle indicating the direction of the external magnetic field measured from the Z-axis of the crystal, α is the angle between the direction of the local quantization axis and the Z-axis of the crystal usually determined by Jahn-Teller distortion [27]. Under the condition $|D1| >> |S_z \cdot (g_1 \cdot H + \lambda_1 \cdot M)|$ in the first approximation, we obtain the following energy states (see Fig. 6 b):

$$\begin{cases} \varepsilon_1^{1,2} = -2D_1 \pm [G_1(T) \cdot \gamma_1], \\ \varepsilon_1^{3,4} = +D_1 \pm [G_1(T) \cdot \gamma_1], \\ \varepsilon_1^{5} = +2D_1, \end{cases} \tag{4}$$

where $G_1(T) = \xi_1 \cdot (g_1 \cdot H + \lambda_1 \cdot M)$ is the temperature-dependent magnetic contribution, ξ_1 is the maximum value of the ion magnetic moment, and $\gamma_1 = cos(\theta + \alpha)$. Considering the contribution of the high-lying levels $\varepsilon_1^{3,4}$ and ε_1^5 to be negligible, only main doublet $\varepsilon_1^{1,2}$ is taken.

Taking into account small rhombic distortions of the $\delta_1(S_x^2 - S_y^2)$ type results in the form of the levels energy:

$$\varepsilon_1^{1,2} = -2D_1 \pm \sqrt{[G_1(T) \cdot \gamma_1]^2 + \delta_1^2}. \tag{5}$$

Basing on this electronic structure of the ion subsystem, and rejecting the contribution from

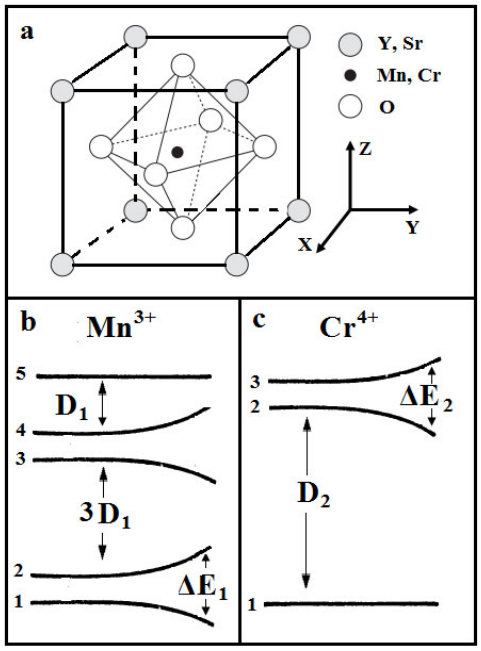

Fig. 6. The unit cell of manganite (a) and the energy structure of the low-lying levels of the Mn^{3+} (b) and Cr^{4+} (c) ions with orthorhombic distortions

high-lying levels, we obtain a well-known result [23]

$$P_1 = \frac{N_1}{4K_BT} \cdot \frac{(\partial \Delta E_1/\partial\theta)^2}{\left[\exp\left(\frac{\Delta E_1}{2K_BT}\right) + \exp\left(-\frac{\Delta E_1}{2K_BT}\right)\right]^2} = \frac{N_1}{16K_BT} \cdot \frac{(\partial \Delta E_1/\partial\theta)^2}{\left[\cosh\left(\frac{\Delta E_1}{2K_BT}\right)\right]^2}, \quad (6)$$

where K_B is Boltzmann constant, $\Delta E_1 = \varepsilon_1^2 - \varepsilon_1^2$.

Satisfactory results for $\Delta H(Mn^{3+})$ were obtained for the following values: $\delta_1 = 1.035 \cdot 10^{-15}$ erg (~ 7.5 K), $G_1(T = 5\text{ K}) = 7.73 \cdot 10^{-15}$ erg (~ 56 K), $M_0 = 499$ G is magnetization at $H = 3.5$ kOe. In the numerical calculation, the temperature dependence of the magnetization (and, consequently, the molecular field) was taken from the experiment (the insert in Fig. 7). This result can be attributed to a single crystallite. For the entire sample, we should average over the angle θ in the range from 0° up to 90°. Fig. 7 (curve 1) shows the calculation result for the contribution of the Mn^{3+} ions subsystem to the line width after averaging (experimental points are plotted there for comparison). The best agreement between the experiment and the calculation is obtained at $\alpha = \pi/6$. This fact indicates the presence of a Jahn–Teller distortion of the octahedron.

3.3. The high-temperature maximum

If we pay attention to the high-temperature maximum depending on the line width, the possible reason for its existence may be the contribution from the Cr^{4+} ion subsystem. This ion has a $3d^2$ configuration and a ^3F electron term with L = 3 and S = 1. In the crystal field of octahedral symmetry, this term splits into a singlet and two low-lying triplets [25]. With a further decrease in symmetry, the main one is the orbital singlet, which has a three-fold spin

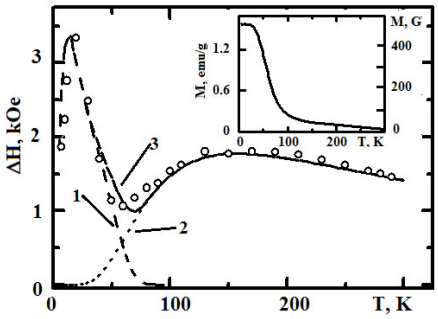

Fig. 7. The temperature dependence of the main resonance line width (curve 1, Fig. 5) of the $Y_{0.5}Sr_{0.5}Cr_{0.5}Mn_{0.5}O_3$ polycrystal. 1 — contribution from the Mn^{3+} ions, 2 — contribution from the Cr^{4+} ions, 3 — resulting curve (calculation). Empty circles correspond to the experiment. The insert shows the temperature dependence of the magnetization taken in the field $H = 3.5$ kOe [12]

degeneracy, and the remaining orbital levels are high-lying and do not significantly affect the state of the main singlet. The spin degeneracy is removed by the spin-orbit interaction and the low symmetric contribution of the crystal field, which results in the quasi-Ising behavior of the Cr^{4+} ion [25]. For such a situation, the spin Hamiltonian is as follows:

$$W_2 = -S_z \cdot (g_2 \cdot H + \lambda_2 \cdot M) \cdot \cos(\theta) - D_2 \cdot \left[S_z^2 - \frac{1}{3} S(S+1) + \delta(S_x^2 - S_y^2) \right], \tag{7}$$

where all designations are given above. Diagonalization of expression (6) under condition $D_2 > 0$ gives eigenvalues:

$$\begin{cases} \varepsilon_1^1 = -2D_2/3, \\ \varepsilon_2^{2,3} = -\dfrac{D_2}{3} \pm \sqrt{[G_2(T) \cdot \gamma_2]^2 + \delta_2^2}, \end{cases} \tag{8}$$

where $G_2(T) = \xi_2 \cdot (g_2 \cdot H + \lambda_2 \cdot M)$ is the temperature - dependent magnetic contribution, ξ_2 is the maximum value of the ion magnetic moment, and $\gamma_2 = \cos(\theta)$.

The scheme of energy levels for low-lying levels of the $3d^2$ configuration is shown in Fig. 6c. In this case, the main level is non-magnetic, and the levels responsible for magnetism are in the excited state. Therefore, when calculating the contribution to the line width from the Cr^{4+} subsystem, it is necessary to take into account the entire set of levels of the spin multiplet. The expression for the P multiplier in equation (2) now has the form:

$$P_2 = \frac{N_2}{4K_BT} \cdot \left(\frac{\partial \Delta E_1}{\partial \theta} \right)^2 \cdot \frac{\exp\left(\dfrac{D_2}{2K_BT}\right) \cdot \left[\exp\left(\dfrac{\Delta E_2}{2K_BT}\right) + \exp\left(-\dfrac{\Delta E_2}{2K_BT}\right) + 4 \right]}{\left[\exp\left(\dfrac{D_2}{2K_BT}\right) + \exp\left(\dfrac{\Delta E_2}{2K_BT}\right) + \exp\left(-\dfrac{\Delta E_2}{2K_BT}\right) \right]^2}. \tag{9}$$

This equation can be easily reduced to

$$P_2 = \frac{N_2}{2K_BT} \cdot \left(\frac{\partial \Delta E_1}{\partial \theta} \right)^2 \cdot \frac{\exp\left(\dfrac{D_2}{2K_BT}\right) \cdot \left[\cosh\left(\dfrac{\Delta E_2}{2K_BT}\right) + 2 \right]}{\left[\exp\left(\dfrac{D_2}{2K_BT}\right) + 2 \cdot \cosh\left(\dfrac{\Delta E_2}{2K_BT}\right) \right]^2}, \tag{10}$$

where $\Delta E_2 = \varepsilon_2^3 - \varepsilon_2^2$, $\delta_2 = 3.45 \cdot 10^{-16}$ erg (~ 2.5 K), $G_2(T = 100\text{ K}) = 9.177 \cdot 10^{-16}$ erg (~ 6.65 K), $M_0 = 5$ G, $D_2 = 3.726 \cdot 10^{-14}$ erg (~ 230 K). Here, as in the previous case, the upper

hemisphere of the angle θ was averaged, but in this case the best results were obtained at $\alpha = 0$. The calculations of the line width $\Delta H(Cr^{4+})$ using the equation (1) with a multiplier (10) are shown in Fig. 7 (curve 2). Curve 3 in Fig. 7 is the sum of two contributions from the Mn^{3+} and Cr^{4+} ion subsystems, and as one can see, there is a good agreement between the calculation and the experiment.

Conclusions

The fine structure in Fig. 3 has a typical form for the Mn^{2+} ion [25]. In our case, the intensity of the fine structure lines is negligible compared to the intensity of absorption by magnetic phases, so the influence of Mn^{2+} ions on the magnetic properties can be ignored. Against the background of line 2, the fine structure lines are not visible. These ions enter as impurities, probably due to non-stoichiometry or distortions on the surface of the crystallites (compare with ref. [19]). This is indirectly indicated by the fact that the lines of the fine structure fall into the resonance region from the core shell, where the maximum distortions of the structure have to take place. The obtained results of magnetic resonance studies are in the satisfactory agreement with the data of magnetostatic measurements [12]. The sample is a set of crystallites interacting with each other at the interface. At the same time, from comparing the temperature dependences of the intensities of the resonant absorption lines 1 and 2 in the region close to the transition ($T_N \approx 80$ K), we can estimate the volume of the core and the outer shell. Since the intensity of the absorption line is proportional to the volume of the magnetic phase, $J_2/J_1 \sim (r^3 - R^3)/R^3$, where r is the outer radius of the granule (crystallite) and R is the radius of the core. The experiment shows that this ratio is $\leqslant 10^{-2}$. For the estimation, let's assume that the granules have a spherical shape, then $r \approx 5 \cdot 10^3$ nm and the shell thickness is $r - R \approx 20$ nm. Analyzing the behavior of the magnetic resonance line width, we can conclude that the low-temperature maximum for line 1 corresponds to the region of magnetic ordering in the crystallite, while the high-temperature maximum enters the paramagnetic region. The set of parameters obtained as a result of fitting the theory to the experiment determines that the molecular field constant for the Mn^{3+} ion subsystem at $T = 5$ K has a value of $\lambda_1 \approx 334.7$, and for the Cr^{4+} ion subsystem its value is $\lambda_2 \approx 7071.2$. These data indicate that a mixed combination of magnetic ion types can be useful in the design of materials with higher magnetic ordering temperatures.

The magnetic resonance spectra were measured by means of the equipment of the Krasnoyarsk Regional Center of Research Equipment of Federal Research Center "Krasnoyarsk Science Center SB RAS". This work was carried out in the framework of the cooperation agreement between the Kazakh National Women's Teacher Training University, Siberian Federal University and L.V. Kirensky Institute of Physics, Krasnoyarsk Scientific Center, Siberian Branch, Russian Academy of Sciences.

References

[1] N.A.Spaldin, S.-W.Cheong, R.Ramesh, Multiferroics: Past, present, and future, *Phys. Today*, **63**(2010), 38–43. DOI: 10.1063/1.3502547

[2] M.Alguero, J.M.Gregg, L.Mitoseriu, Nanoscale Ferroelectrics and Multiferroics: Key Processing and Characterization Issues, and Nanoscale Effects, John Wiley & Sons Ltd, 2016. DOI: 10.1002/9781118935743

[3] E.Dagotto, Nanoscale phase separation and colossal magneto-resistance. The physics of manganites and related compounds, Springer, 2003. DOI: 10.1007/978-3-662-05244-0

[4] C.Moure, O.Pena, Magnetic features in $REMeO_3$ perovskites and their solid solutions (RE=rare-earth, Me=Mn, Cr), *J. Magn. Magn. Mater.*, **337-338**(2013), 1–22. DOI: 10.1016/j.jmmm.2013.02.022

[5] T.Bora, S.Ravi, Sign reversal of magnetization and exchange bias field in $LaCr_{0.85}Mn_{0.15}O_3$, *J. Appl. Phys.*, **114**(2013), 183902. DOI: 10.1063/1.4826903

[6] C.L.Li, S.Huang, X.X.Li, C.M.Zhu, G.Zerihun, C.Y.Yin, C.L.Lu, S.L.Yuan, Negative magnetization induced by Mn doping in $YCrO_3$, *J. Magn. Magn. Mater.*, **432**(2017) 77–81. DOI: 10.1016/j.jmmm.2017.01.078

[7] N.Kallel, M.Hazzez, N,Ihzaz, Cryvstal Structure, Magnetic and Electrical Properties of Half-Doped Chromium Manganite $La_{0.5}Sr_{0.5}Mn_{0.5}Cr_{0.5}O_3$, *J. Supercond. Nov. Magn.*, **32**(2019), 2623. DOI: 10.1007/s10948-019-4997-4

[8] A.Kumar, S.M.Yusuf, The phenomenon of negative magnetization and its implications, *Phys. Rep.*, **556**(2015), 1–34. DOI: 10.1016/j.physrep.2014.10.003

[9] M.R.Ibarra, P.A.Algarabel, C.Marquina, J.Blasco, J.Garcia, Large Magnetovolume Effect in Yttrium Doped La-Ca-Mn-O Perovskite, *Phys. Rev. Lett.*, **75**(1995), 3541. DOI: 10.1103/PhysRevLett.75.3541

[10] R.S.Freitas, L.Ghivelder, F.Damay, F.Dias, L.F.Cohen, Magnetic relaxation phenomena and cluster glass properties of $La_{0.7-x}Y_xCa_{0.3}MnO_3$ manganites, *Phys. Rev. B*, **64**(2001), 144404. DOI: 10.1103/PhysRevB.64.144404

[11] J.Dho, W.S.Kim, N.H.Hur, Reentrant Spin Glass Behavior in Cr-Doped Perovskite Manganite, *Phys. Rev. Lett.*, **89**(2002), 027202. DOI: 10.1103/PhysRevLett.89.027202

[12] G.S.Patrin, M.M.Mataev, K.Zh.Seitbekova, Ya.G.Shiyan, S.A.Yarikov, S.M.Zharkov, Magnetic and Resonance Properties of the $Y_{0.5}Sr_{0.5}Cr_{0.5}Mn_{0.5}O_3$ Polycrystal, *Phys. Sol. State*, **62**(2020), 1350–1354. DOI: 10.1134/S1063783420080272

[13] M.M.Mataev, G.S.Patrin, K.Zh.Seitbekova, Zh.Y.Tursinova, M.R.Abdraimova, Synthesis and Analysis of Chromium and Calcium Doped $YMnO_3$, *Orient. J. Chem.*, **35**(2019), 1162. DOI: 10.13005/ojc/350335

[14] Ch.P.Poole, Electron Spin Resonance, Interscience Publishers, 1967.

[15] M.A.Lopez-Quintela, L.E.Hueso, J.Rivas, F.Rivadulla, Intergranular magnetoresistance in nanomanganites, *Nanotechnology*, **14**(2003), 212. DOI: 10.1088/0957-4484/14/2/322

[16] Ll.Balcells, J.Fontcuberta, B.Martinez, X.Obradors, High-field magnetoresistance at interfaces in manganese perovskites, *Phys. Rev. B*, **58**(1998), R14697(R). DOI: 10.1103/PhysRevB.58.R14697

[17] L.E.Hueso, P.Sande, D.R.Miguens, J.Rivas, F.Rivadulla, M.A.Lopez-Quintela, Tuning of the magnetocaloric effect in $La_{0.67}Ca_{0.33}MnO_{3-\delta}$ nanoparticles synthesized by sol–gel techniques, *J. Appl. Phys.*, **91**(2002), 9943–9947. DOI: 10.1063/1.1476972

[18] J.Curiale, M.Granada, H.E.Troiani, R.D.Sanchez, A.G.Leyva, P.Levy, K.Samwer, Magnetic dead layer in ferromagnetic manganite nanoparticles, *Appl. Phys. Lett.*, **95**(2009), 043106. DOI: 10.1063/1.3187538

[19] M.P. de Jong, I.Bergenti, V.A.Dediu, M.Fahlman, M.Marsi, C.Taliani, Evidence for Mn^{2+} ions at surfaces of $La_{0.7}Sr_{0.3}MnO_3$ thin films, *Phys. Rev. B*, **71**(2005), 014434. DOI: 10.1103/PhysRevB.71.014434

[20] I.S.Poperechny, Yu.L.Raikher, Ferromagnetic resonance in uniaxial superparamagnetic particles, *Phys. Rev. B*, **93**(2016), 014441. DOI: 10.1103/PhysRevB.93.014441

[21] V.Krivoruchko, T.Konstantinova, A.Mazur, A.Prokhorov, V.Varyukhin, Magnetic resonances spectroscopy of nanosize particles $La_{0.7}Sr_{0.3}MnO_3$, *J. Magn. Magn. Mater.*, **300**(2006), e122–125. DOI: 10.1016/j.jmmm.2005.10.163

[22] B.H.Clarke, Resonance relaxation in $Mn_xFe_yO_4$ by slow relaxing manganic and ferrous ions, *J. Phys, Chem. Solids*, **27**(1966), 353–362. DOI: 10.1016/0022-3697(66)90042-4

[23] A.G.Gurevich, G.A.Melkov, Magnetization Oscillations and Waves, CRC Press, Inc., 2000.

[24] A.M.Clogston, Relaxation phenomena in ferrites, *Bell. System Tech. J.*, **34**(1955), 739. DOI: 10.1002/j.1538-7305.1955.tb03774.x

[25] A.Abragam, B.Bleany, Electron paramagnetic resonance of transition ions, Clar. Press, 1970.

[26] V.Markovich, A.Wisniewski, H.Szymczak, Chapter One - Magnetic Properties of Perovskite Manganites and Their Modifications, In: Handbook of Magnetic Materials, vol. 22, Elsevier, 2014. DOI: 10.1016/B978-0-444-63291-3.00001-5

[27] K.I.Kugel', D.I.Khomskii, The Jahn-Teller effect and magnetism: transition metal compounds, *Sov. Phys. Usp.*, **25**(1982), 231–256. DOI: 10.1070/PU1982v025n04ABEH004537

Резонансные свойства поликристалла $Y_{0.5}Sr_{0.5}Cr_{0.5}Mn_{0.5}O_3$

Мухаметкали М. Матаев
Казахский национальный женский педагогический университет
Алматы, Казахстан

Геннадий С. Патрин
Сибирский федеральный университет
Институт физики им. Л. В. Киренского
Федеральный исследовательский центр КНЦ СО РАН
Красноярск, Российская Федерация

Карима Ж. Сейтбекова
Казахский национальный педагогический университет им. Абая
Алматы, Казахстан

Ярослав Г. Шиян
Сибирский федеральный университет
Институт физики им. Л В. Киренского
Федеральный исследовательский центр КНЦ СО РАН
Красноярск, Российская Федерация

Виктор Р. Чуркин
Сибирский федеральный университет
Красноярск, Российская Федерация

Аннотация. В работе представлены результаты экспериментальных исследований магниторезонансных свойств поликристаллической системы $Y_{0.5}Sr_{0.5}Cr_{0.5}Mn_{0.5}O_3$. Получено, что области магнитного упорядочения при $T < 80$ К в спектре наблюдается две линии поглощения. При переходе в парамагнитную область одна из линий исчезает, но появляются набор слабых линий, идентифицируемых как принадлежащие примесным ионам Mn^{2+}. В рамках теории одноионной релаксации проведен анализ температурного поведения ширины линии основного пика. Установлено, что за низко температурный пик ответственны ионы Mn^{3+}, а за высокотемпературный — ионы Cr^{4+}. Определены константы молекулярных полей, действующих на подсистемы ионов Mn^{3+} и Cr^{4+}.

Ключевые слова: иттрий-стронциевый хромито-манганит, антиферромагнитное взаимодействие, магнитный резонанс, одноионная релаксация.